

# Characterization of the 15-5 Stainless Steel Electric Discharge Machining Recast Layer

A Senior Project

presented to

the Faculty of the Materials Engineering Department  
California Polytechnic State University, San Luis Obispo

In Partial Fulfillment

of the Requirements for the Degree

Bachelor of Science, Materials Engineering

by

Rhys Gilmore, Julian Lohser

Advisor: Prof. Blair London

Sponsor: Aerojet Rocketdyne

June, 2017

## Abstract

Electric discharge machining (EDM) is a non-conventional machining process that is used for tough, hard materials or materials that require no tool force. Wire EDM produces a recast layer and heat-affected zone as a result of rapid melting and quenching at the surface of the cut. A secondary machining operation has been required to remove this layer. Previous estimates of the depth of the recast layer are likely too conservative due to improvements in the technology; therefore, the goal of this study is to characterize and more accurately investigate the size of the layer. Two EDM machine parameters, voltage and pulse on-time, were varied for the machining of 15-5 PH stainless steel. Three levels of each factor were investigated: recommended machine settings, -25%, and -50%. Average recast layer thickness was evaluated using a scanning electron microscope (SEM). Microhardness testing was also performed on ground, polished, and etched samples. Compared to previous studies and industry specifications, the recast layer was significantly smaller or not observed at all. SEM imaging generally indicated an oxide layer with porosity and microcracking near the surface. Microhardness results showed no difference between the surface and base material at maximum voltage, but significant difference between recast layer and base material for all lower voltages. However, a secondary machining operation is still recommended to remove any recast or oxide layers, but less material must be removed than prior industry estimates.

**Keywords:** Electric Discharge Machining, Recast Layer, Microhardness, Stainless Steel, Scanning Electron Microscopy, Materials Engineering

## Acknowledgements

We would like to acknowledge Christopher Shipley at *Aerojet Rocketdyne* for his wealth of information and assistance as the project transformed. We would also like to thank Professor Blair London of the Cal Poly Materials Engineering Department for his guidance and advice throughout the project.

## Table of Contents

Abstract .....	i
Acknowledgements .....	ii
List of Figures .....	iv
List of Tables .....	v
I. Introduction .....	1
i. Background .....	1
ii. Alloy Information .....	1
iii. Electric Discharge Machining .....	2
iv. EDM History .....	3
v. Wire-cut versus Sinker EDM .....	5
vi. Dielectric Fluid .....	5
vii. EDM Sparking .....	6
viii. Surface Produced .....	7
ix. EDM Recast Layer .....	7
II. Experimental Procedure .....	8
III. Results .....	11
i. Microhardness .....	11
ii. Recast Layer Thickness .....	13
IV. Discussion .....	14
i. Microhardness .....	14
ii. Recast Layer Thickness .....	15
V. Conclusions .....	17
Works Cited .....	18

## List of Figures

Figure 1: 15-5 is commonly used in flanges for aerospace components. <sup>2</sup> .....	2
Figure 2: Rough cut wire electric discharge machining process being performed on a metallic material. <sup>9</sup> .....	3
Figure 3: Early EDM experiment of US scientists; the electrode is attached to a movable quill. <sup>7</sup>	4
Figure 4: A diagram depicting the process by which the sparking occurs between the electrode and the workpiece during the EDM process. <sup>11</sup> .....	6
Figure 5: SEM images of rough surface of steel immediately following the EDM process. <sup>16</sup> .....	7
Figure 6: Large recast layer from experiment performed in 2005. <sup>16</sup> .....	8
Figure 7: Microstructure of the surface of IN-718 post-EDM, depicting the depth of the recast layer and HAZ. <sup>11</sup> .....	8
Figure 8: 15-5 PH bar stock was bisected with EDM for this experiment. ....	9
Figure 9: Example recast layer thickness measurements on 8V, 13 $\mu$ s on-time samples.....	10
Figure 10: Effects of on time, voltage on the hardness (HV) of the recast layer.....	11
Figure 11: (a) 6V, 13 $\mu$ s on-time, blunted indenter near recast layer. (b) 4V, 7 $\mu$ s on-time, microhardness test performed directly on crack. ....	12
Figure 12: Average calculated recast layer thicknesses overlaid on representative SEM images for each sample. ....	13
Figure 13: A 13 $\mu$ s, 8V sample exhibits variability in recast layer thickness.....	16

## List of Tables

Table I: Mechanical Properties of 15-5 PH.....	1
Table II: Composition of 15-5 Stainless Steel.....	2
Table III: Experimental Design.....	9
Table IV: Average Microhardness Data for EDM Samples.....	11
Table V: P Values for Difference Between Hardness Readings.....	12
Table VI: ANOVA Analysis of Parameter Effect On Recast Thickness.....	14

# I. Introduction

## i. Background

*Aerojet Rocketdyne* designs and manufactures rocket engines for government clients such as NASA and the Air Force. The company has developed numerous groundbreaking engines, such as the F-1 for the Saturn V and the RS-25 for the Space Shuttle. Due to the high temperature and stress encountered during operation, rocket engines require advanced alloys and precise geometries. Non-conventional machining techniques, such as electric discharge machining (EDM), are increasingly relevant because these alloys are too tough and hard for conventional machining. Industry partner *Aerojet Rocketdyne* requires information regarding the effects of the EDM recast layer on 15-5 precipitation hardenable stainless steel. It is known that increased surface roughness caused by the EDM recast layer can negatively affect mechanical properties, notably fatigue strength. As a result, a secondary machining operation is required to eliminate the recast layer. However, as the EDM process has improved technologically, the recast layer thickness has reduced. Prior estimates of the recast layer thickness are likely too conservative. *Aerojet Rocketdyne* requires a modern characterization of the EDM recast layer to investigate its size and potential effects.

## ii. Alloy Information

15-5 (15% chromium, 5% nickel) is a martensitic, precipitation hardenable stainless steel useful for its high strength, good corrosion resistance, and relatively high temperature use. This alloy is similar to the most common precipitation hardenable stainless steel, 17-4, except it lacks the ferrite phase. Like 17-4, 15-5 is weldable with common fusion and resistance techniques. Its mechanical properties are generally favorable (Table I). As a result of its advantageous properties, 15-5 finds versatile use in the aerospace, chemical, and food processing industries (Figure 1).

Table I: Mechanical Properties of PH 15-5<sup>1</sup>

<i>Tensile Strength</i>	190 ksi
<i>Yield Strength</i>	175 ksi
<i>Elongation</i>	9 %
<i>Hardness</i>	43 HRC



Figure 1: 15-5 is commonly used in flanges for aerospace components.<sup>2</sup>

Stainless steels are typically classified by their microstructure: austenitic, martensitic, ferritic, duplex, or precipitation hardenable. Although 15-5 is martensitic, it is classified as precipitation hardenable because precipitates are its primary strengthening mechanism. The iron-nickel martensite structure is body centered cubic. During aging, copper compounds form precipitates within the martensitic matrix. These precipitates effectively inhibit dislocation movement, increasing strength.<sup>3</sup>

The composition of the alloy includes a significant amount of chromium, which enhances the corrosion resistance of the alloy (Table II).

Table II: Composition of 15-5 Stainless Steel<sup>1</sup>

<i>wt%</i>	<b>C</b>	<b>Si</b>	<b>Mn</b>	<b>P+S max</b>	<b>Cr</b>	<b>Ni</b>	<b>Cu</b>	<b>Nb</b>	<b>Fe</b>	<b>Mo</b>
<b>15-5</b>	0.07	1.0	1.0	0.03P 0.015S	14.0-15.50	3.50-4.50	2.50-4.50	0.45	Bal	0.50

Stainless steels typically have at least 12% chromium to provide corrosion resistance. 15-5 forms the BCC iron-nickel martensite structure. A low carbon content ensures the martensite is not too strained or brittle, like that of plain carbon steels. The copper atoms form the precipitates, contributing to the high strength of the alloy.

### iii. Electric Discharge Machining

Electrical Discharge Machining (EDM) is the process of machining electrically conductive materials by using precisely controlled sparks that occur between an electrode and a workpiece



in the presence of a dielectric fluid (Figure 2). The electrode may be considered the cutting tool.<sup>7</sup> EDM is a thermoelectric process. Loss of material from the workpiece occurs due to the high heat produced by the electrical discharge between the electrode and the workpiece. The removed material then forms a chip in the dielectric fluid. EDM is different than most chip-making machining, because the electrode does not physically contact the workpiece during material removal. This means that EDM has no tool force, making it preferable for complex geometries.<sup>7</sup> Due to the large heat generation in EDM, melting and evaporation can occur at the surface of the workpiece, and the rapid cooling that follows forms a detrimental recast layer. This recast layer has significantly different properties compared to the parent structure, and many micro-cracks due to the thermal and tensile stress during the rapid cooling process. This leads to a reduction in fatigue properties of the metal.<sup>8</sup> In most applications, the reduction in fatigue strength properties means that a secondary machining operation must be performed on the workpiece to remove the layer.

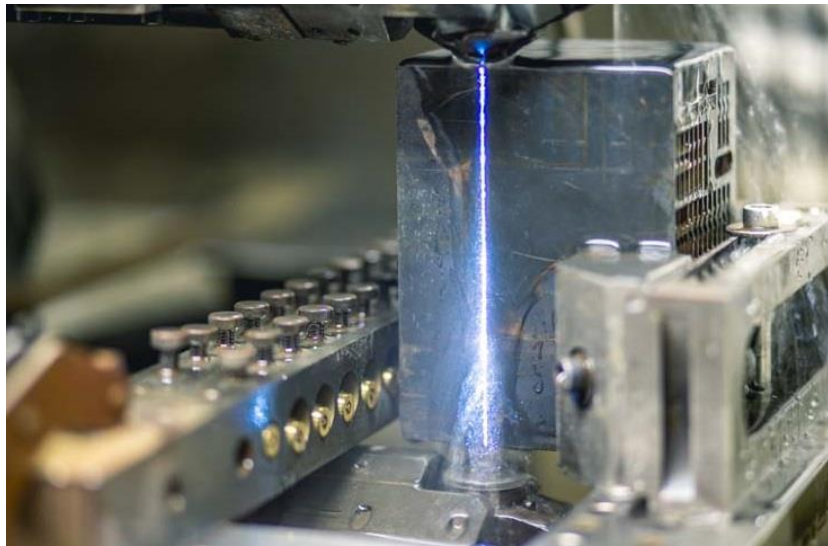


Figure 2: Rough cut wire electric discharge machining process being performed on a metallic material.<sup>9</sup>

#### iv. EDM History

Sinker EDM was developed in the beginning of World War II, by both the USSR and the USA. The USSR discovered EDM in their attempt to suppress sparking between tungsten used as electrical contact material and other metals. They immersed the tungsten in oil, which did not suppress sparking, but they realized that it allowed for predictable sparking compared to air.

Through further experimentation, they discovered that the sparks could be used to remove material from the tungsten. They used resistors and capacitors in their system, thus earning the name R-C type EDM. The R-C type EDM system they developed to control material removal is still in use today.<sup>7</sup>

At the same time, scientists in the US discovered EDM in their attempt to erode taps and drills that were breaking inside hydraulic valves with aluminum bodies. They initially produced an etching tool that involved placing an electrode on the material to be removed, and lifting it away. This produced a spark that removed material, but their process was too slow to be useful. They increased the power, and started using water to remove the material. This made the process practical, but to make it more efficient, they decided to automate it. The system they developed involved a movable quill with an electrode attached, and an electromagnet above it. When electricity was flowing, the electromagnet would pull the quill up, bringing the electrode with it (Figure 3). The separation of the electrode and workpiece caused sparking. Once the electrode was far enough from the workpiece, the electricity would shut off, allowing the quill to fall, and return the electrode to the surface of the workpiece, repeating the process. While their exact process is not used today, the American scientists showed that sparking could occur thousands of times per second.

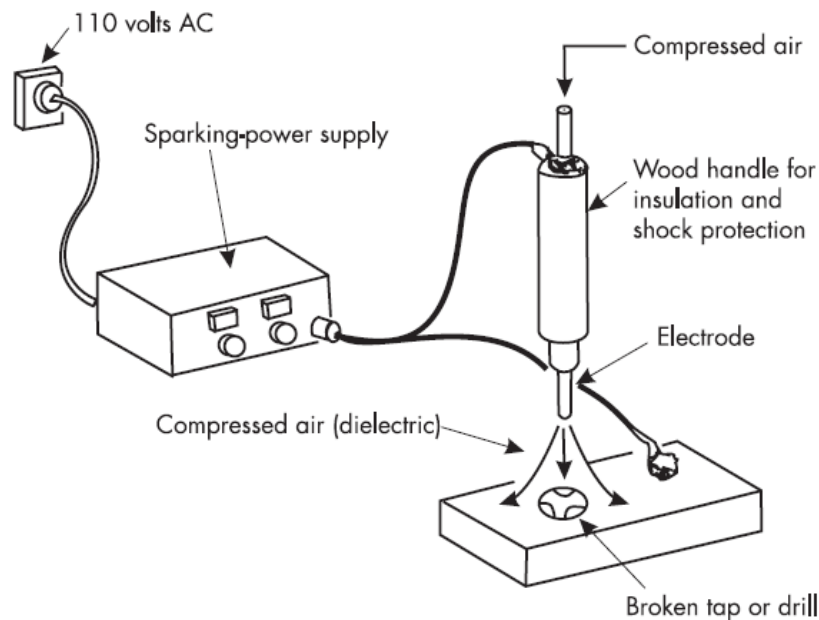


Figure 3: Early EDM experiment of US scientists; the electrode is attached to a movable quill.<sup>7</sup>

Wire-cut EDM was developed sometime in the early 60s or early 70s, as a solution to the labor-intensive and expensive sinker EDM. Stationary wire was considered at first, but spark erosion meant that the wire would be easily broken. The solution was to have a continuously traveling wire. However, this process did not become practical until the arrival of a series of technological advancements, like computer-numerical control, ball screws, and servo motors in the early 70s.

#### v. Wire-cut versus Sinker EDM

Both wire-cut and sinker EDM use sparking to remove material. Wire EDM (WEDM) is a process in which the electrode is a continuously moving electrically conductive wire, while sinker EDM is a single electrode.<sup>10</sup> WEDM has a better material removal rate than sinker EDM. However, sinker EDM is better at producing three-dimensional shapes, because the wire used for WEDM must pass through the workpiece being machined. WEDM does not usually submerge the workpiece in dielectric fluid, while in sinker EDM, the workpiece is submerged.

#### vi. Dielectric Fluid

The Dielectric fluid used in EDM machines provides important functions in the EDM process. The fluids provide a known electrical barrier between the electrode and workpiece, cooling for the electrode, workpiece, and vaporized material that becomes the EDM chip, and removal of the EDM chip. A dielectric fluid is an electrical insulator that resists electricity until a high enough voltage is applied, at which point it becomes an electrical conductor. The applied voltage at which the fluid changes is called the ionization point. The ionization point occurs locally in the fluid, meaning only the area that the voltage is applied to will become conductive, while the rest of the dielectric fluid remains an insulator. This allows for the controlled sparking between the electrode and workpiece, because the voltage potential can be applied to the area to be removed, leaving the rest of the workpiece insulated from the electricity.

Dielectric fluids are generally either hydrocarbon oil or deionized water. The deionized water has any electrically conductive impurities removed. In general, wire cut EDM machines use deionized water, while plunge machines use hydrocarbon oil, but wire cut sometimes uses hydrocarbon oils as well. Hydrocarbon fluids maintain their electrical integrity throughout the machining process, making them the fluid of choice for submerged machining. On the other

hand, deionized water readily absorbs materials that can change its ionization point and conductivity, such as material removed from the workpiece or the electrode. To counteract this, a high velocity flow of fresh deionized water over the workpiece is used.

#### vii. EDM Sparking

Sparking occurs as the electrode moves across the workpiece. The electrode removes material until a prescribed distance between the electrode and workpiece is reached, and then it moves onto the next area, which can be seen in Figure 5. Sparking occurs at 2-500 kHz.<sup>7</sup> The ionization

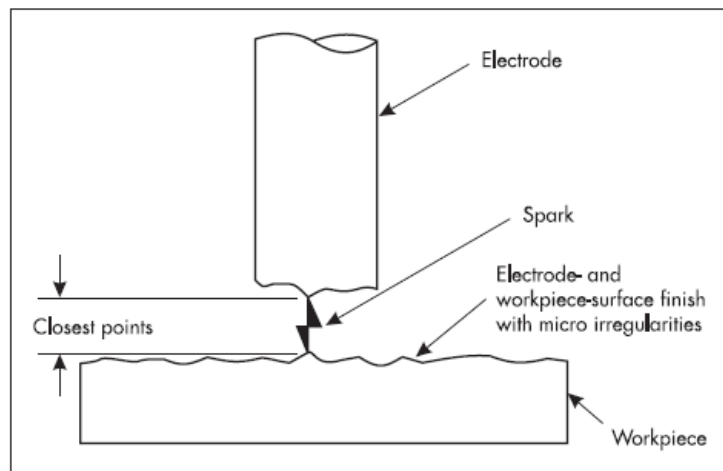


Figure 4: A diagram depicting the process by which the sparking occurs between the electrode and the workpiece during the EDM process.<sup>11</sup>

point of the dielectric fluid determines the sparking voltage. Workpieces with high melting temperatures will have less material removed per spark than those with lower melting temperatures. Sparking also produces a significant temperature gradient in the workpiece. There are five main temperature zones that should be considered; the first is the surface that gets hot enough to be vaporized. The second temperature zone is partially part of the first zone, because they are small amounts of vapor that are separated from the main cloud; these do not have any effect on properties. The third zone is material that is melted, but does not get hot enough to escape from the surface, and thus re-solidifies. The fourth and fifth zones are similar in that they both experience heat that is not enough to melt them, but differ in responses to the heat. The material in the fourth temperature zone may experience enough heat to change some properties, but the material in the fifth zone experiences so little heat it is considered the beginning of the parent material. The first, third, and fourth zones are often combined in literature and referred to as the heat-affected zone (HAZ).<sup>12</sup>

### viii. Surface Produced

The surface of any electro-discharge machined workpiece appears as a distribution of craters.<sup>13</sup> The size of craters, and the quality of the workpiece, are mainly controlled by the melting temperature of the workpiece, electrical power, and the amount of time the electrical power is applied to the workpiece. The structure of the electrode also plays a significant role. The surface condition of the electrode will be reproduced on the machined surface of the workpiece. The surface is a combination of redeposited and re-solidified layers. Re-deposited layers form from the small amounts of EDM chips that are close enough to the surface to re-deposit themselves. Figure 5 shows how rough the surface produced can be. Re-solidified layers are formed where the workpiece gets hot enough to melt, but is still unable to separate from the surface. When the spark is turned off, it re-solidifies.

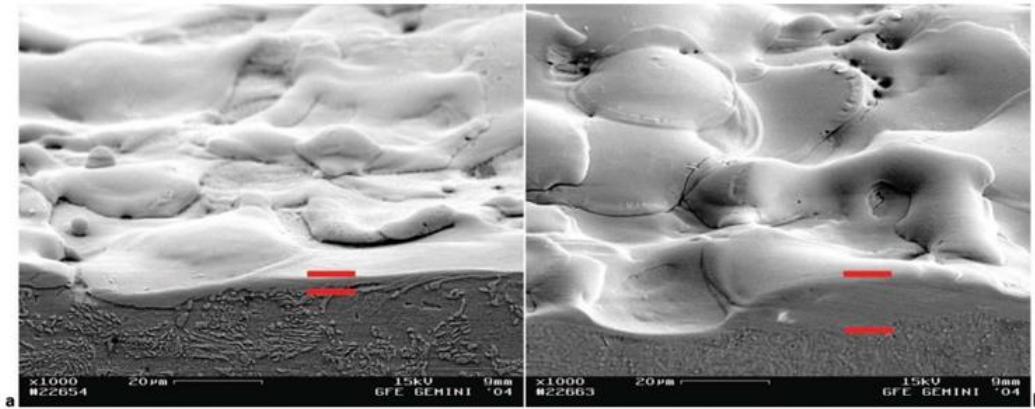


Figure 5: SEM images of rough surface of steel immediately following the EDM process.<sup>16</sup>

### ix. EDM Recast Layer

Recast layers form due to the combination of the re-deposited layer and the re-solidified layer. The recast layer formed is thus composed of re-solidified metallic materials, elements of the electrode material, and oxides and other byproducts of the dielectric fluid.<sup>14</sup> When working with steel, if enough carbon is accumulated, the rapid cooling once the spark is turned off can cause the recast layer to form martensite.<sup>15</sup> Recast layers have a high propensity to cracking when subjected to fatigue loads. The recast layer used to be much larger, as seen in Figure 6.

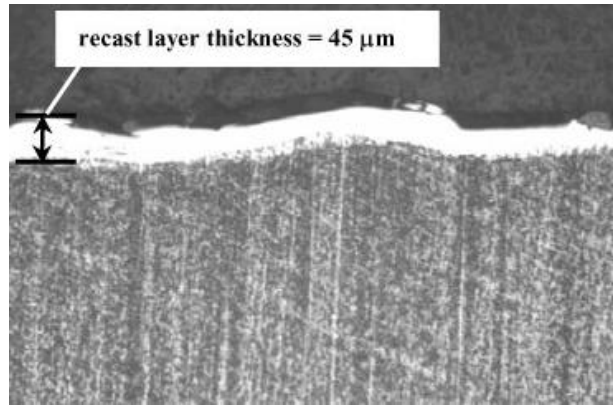


Figure 6: Large recast layer from experiment performed in 2005.<sup>16</sup>

There are considerably more defects when compared to the parent microstructure, which can be seen in Figure 7. The recast layer seen in this image is somewhat small because this work was done recently. The heat affected zone is of average depth. These all act as sites for crack propagation, causing the material to fail due to multiple, smaller cracks, rather than one large crack.<sup>5</sup> Due to the rough surface produced, the recast layer is extremely detrimental to the mechanical properties of materials and must be removed. Removal is usually performed using a chemical etching process, or by polishing.

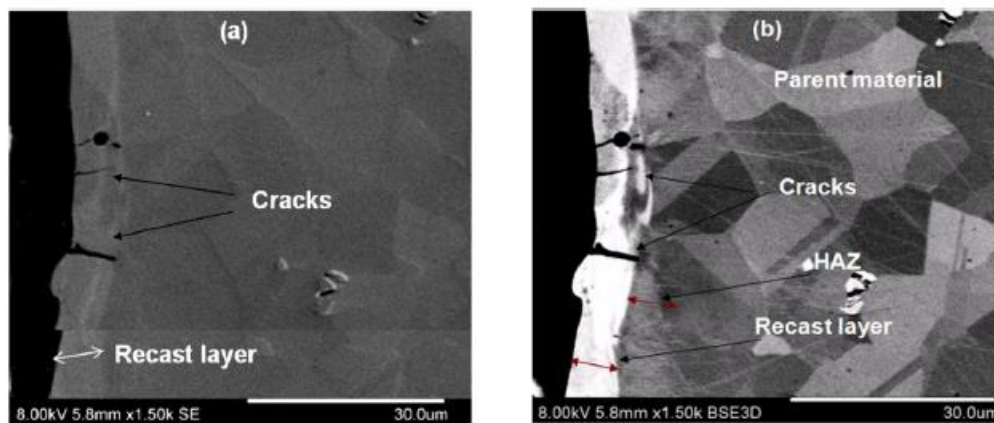


Figure 7: Microstructure of the surface of IN-718 post-EDM, depicting the depth of the recast layer and HAZ.<sup>11</sup>

## II. Experimental Procedure

Two six foot lengths of 0.5" diameter rods of 15-5 precipitation hardenable martensitic stainless steel were obtained for this study. Rods were sectioned into 6" lengths and bisected with electric

discharge machining at varying levels of pulse on-time and peak voltage (Figure 8). Both pulse on-time and peak voltage were set at the manufacturer recommended specifications initially. The recommended setting was 8V peak voltage and 13 μs on-time. These parameters were then reduced by 25% and 50%, to obtain a three-by-three test matrix (Table III).

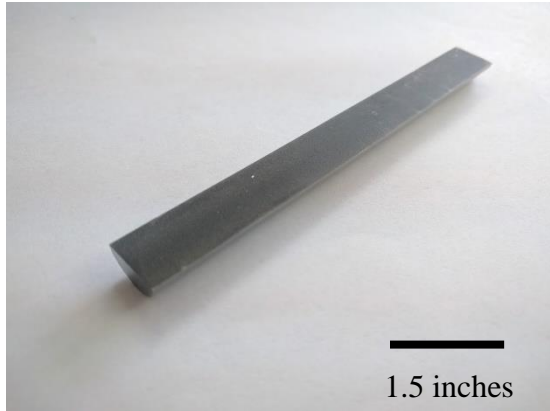


Figure 8: 15-5 PH bar stock was bisected with EDM for this experiment.

Table III: Experimental Design

	8 V	6 V	4 V
<b>Pulse on-time</b> 13 μs			
<b>Pulse on-time</b> 10 μs			
<b>Pulse on-time</b> 7 μs			

The 6” lengths were sectioned into metallography specimens and nickel plated using Buehler Edgemet electro-less nickel plating solution to retain the recast layer, as well as provide lateral support for microhardness testing directly on the layer. Samples were then mounted in Bakelite, ground, and polished to a 0.5 μm diamond finish. After polishing, some samples were etched with glyceresia.

Microhardness measurements were performed on the polished samples using a microhardness indenter across the recast layer, as well as into the base metal. The indenter was used at 500 kgf. The diagonals of the diamond indent were measured. The Vickers hardness (HV) was then determined from Equation 1, where D is the average of the two diagonals, and the load is in Newtons.

$$\text{Equation 1: } HV = 0.1891 * \left( \frac{\text{Load}}{D^2} \right)$$

A minimum of four readings were obtained per sample for both the recast layer and base material.

Scanning electron microscopy was performed using an FEI Quantum 400 with an Everhart-Thornley detector for topography, and backscatter detector for compositional analysis. Representative images of the recast layer at magnifications varying from 40x-3500x were taken for at least two samples per sample group. Backscatter images were used to confirm the boundary between nickel plating and recast layer. Recast layer thicknesses were calculated using these images.

Recast layer thicknesses for each sample group were calculated from microscopy images. Because no technical standard for measuring average recast thickness exists, a method was adapted from a similar study (Figure 9).

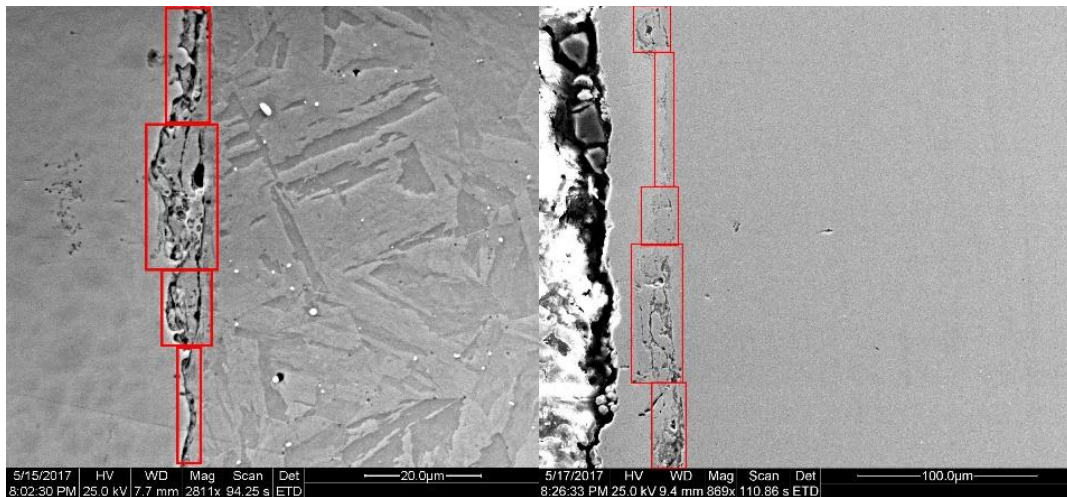


Figure 9: Example recast layer thickness measurements on 8V, 13 µs on-time samples.

Rectangles were drawn around areas of similar thicknesses, and a weighted average thickness, measured by the width and weighted by the length, was calculated. Calculations were performed on multiple SEM images at varying magnifications to obtain weighted recast layer thickness values for each sample group.



### III. Results

#### i. Microhardness

Microhardness testing was conducted to investigate the difference in hardness between the base material and the recast layer. Tests were performed across the recast layer as well as into the base material to produce average hardness values for the base material and the recast layer (Table IV).

Table IV: Average Microhardness Data for EDM Samples

	8 V	6 V	4 V
<b>Pulse on-time</b>	BASE: <b>342.9 HV</b>	BASE: <b>364.7 HV</b>	BASE: <b>354.1 HV</b>
<b>13 <math>\mu</math>s</b>	RECAST: <b>349.9 HV</b>	RECAST: <b>307.3 HV</b>	RECAST: <b>295.7 HV</b>
<b>Pulse on-time</b>	BASE: <b>338.0 HV</b>	BASE: <b>368.5 HV</b>	BASE: <b>347.1 HV</b>
<b>10 <math>\mu</math>s</b>	RECAST: <b>324.2 HV</b>	RECAST: <b>308.4 HV</b>	RECAST: <b>311.1 HV</b>
<b>Pulse on-time</b>	BASE: <b>334.1 HV</b>	BASE: <b>355.2 HV</b>	BASE: <b>342.8 HV</b>
<b>7 <math>\mu</math>s</b>	RECAST: <b>308.6 HV</b>	RECAST: <b>338.6 HV</b>	RECAST: <b>294.6 HV</b>

A two-sample t-test was performed to investigate the statistical significance of the difference between the recast and base material hardness values for each sample. Main effect plots for on time and voltage were produced (Figure 10).

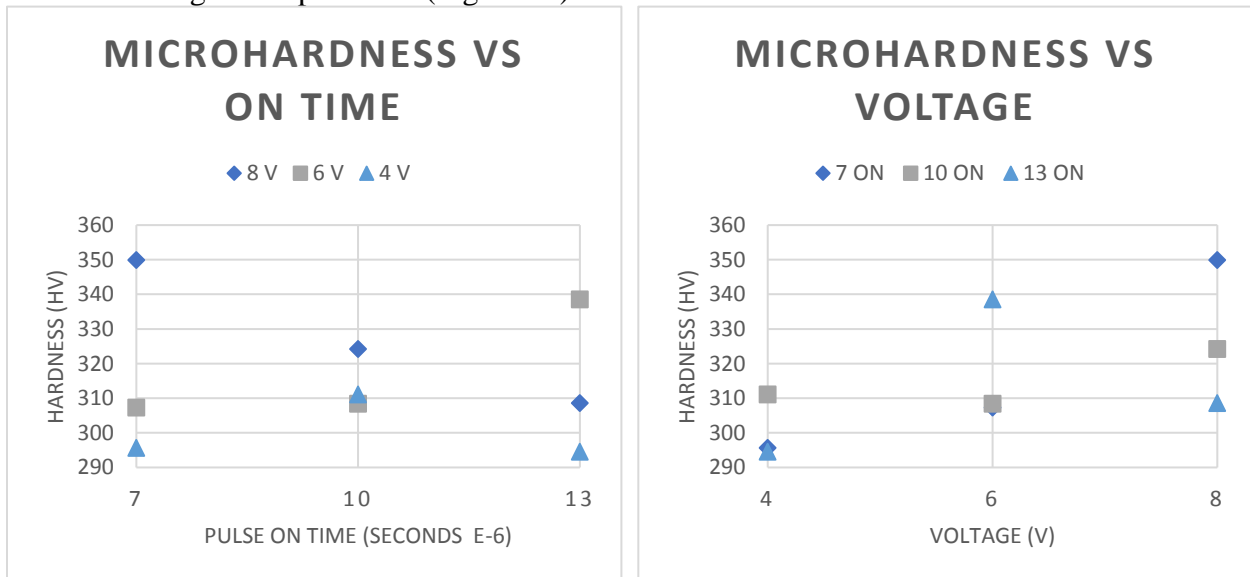


Figure 10: Effects of on time, voltage on the hardness (HV) of the recast layer.

At an  $\alpha$  level of 0.05, this analysis indicates there is a significant difference for samples below the maximum voltage (Table V).

Table V: P Values for Difference Between Hardness Readings

	8 V	6 V	4 V
<b>Pulse on-time</b>			
<b>13 <math>\mu</math>s</b>	0.651	0.001	0.012
<b>Pulse on-time</b>			
<b>10 <math>\mu</math>s</b>	0.449	0.006	0.037
<b>Pulse on-time</b>			
<b>7 <math>\mu</math>s</b>	0.254	0.036	0.002

However, microscopy suggests that testing may have produced unreliable data. Micrographs depict blunting near the indent towards the recast layer, indicating that it may be harder than the base material (Figure 11). Due to the prevalence of cracks in the recast layer, some microhardness tests were performed on cracks, which may have led to reduced hardness readings as well.

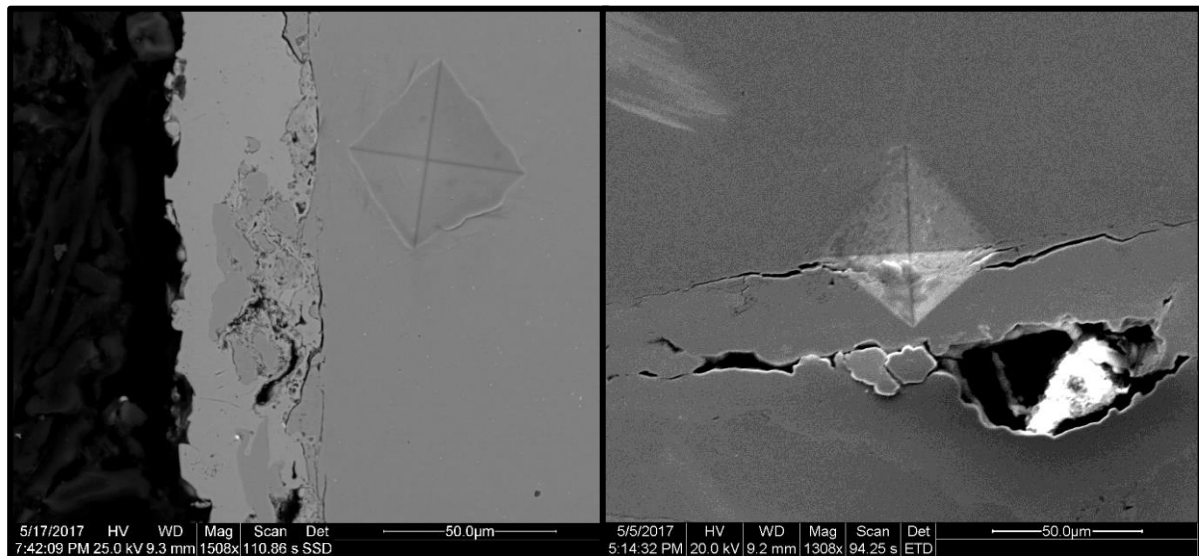


Figure 11: (a) 6V, 13  $\mu$ s on-time, blunted indenter near recast layer. (b) 4V, 7  $\mu$ s on-time, microhardness test performed directly on crack.

Microhardness indents in areas of equal hardness should produce a diamond with equal side lengths.

## ii. Recast Layer Thickness

Using the rectangle weighted average method, recast layer thicknesses were measured for each sample group (Figure 12).

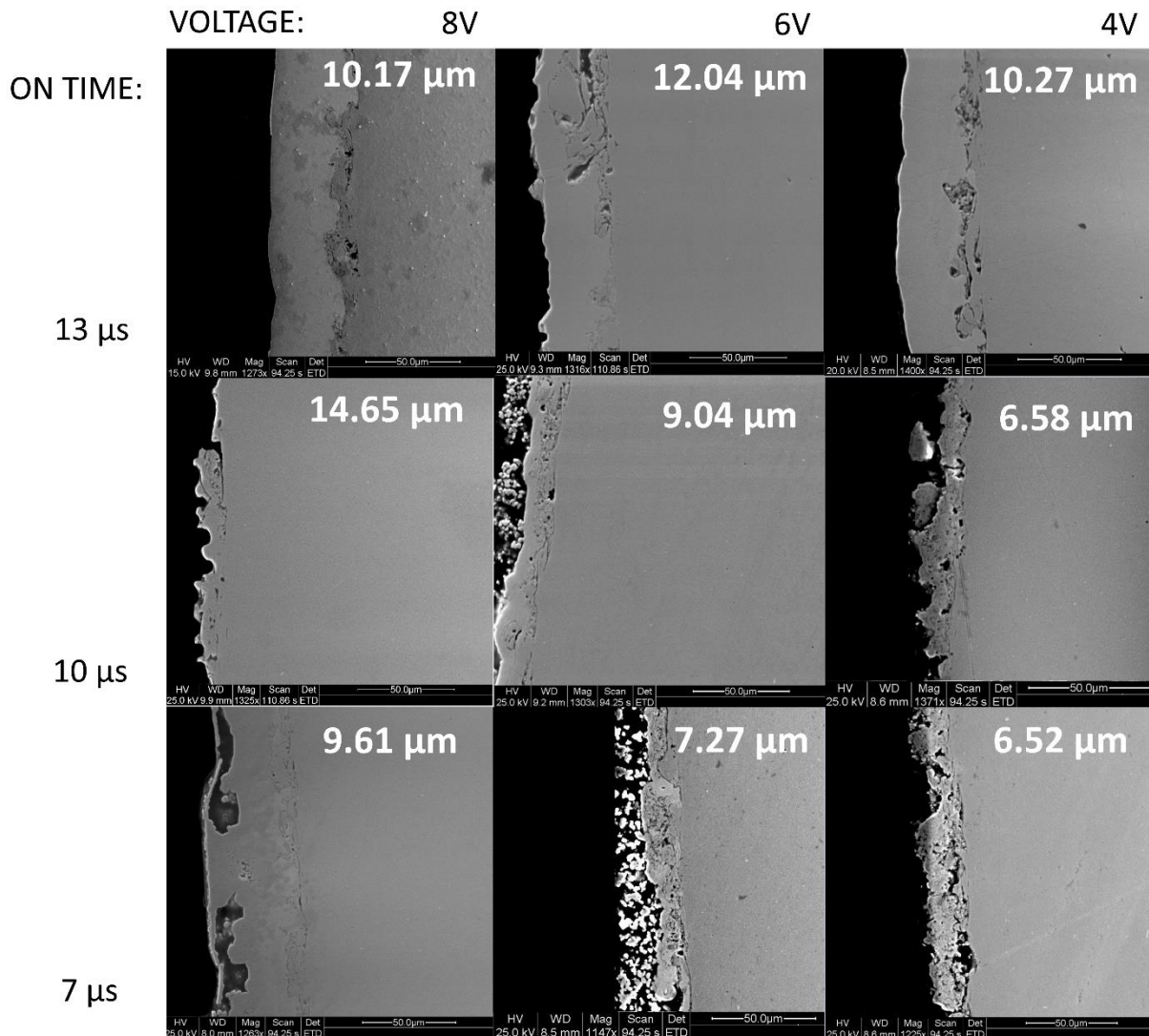


Figure 12: Average calculated recast layer thicknesses overlaid on representative SEM images for each sample.

Statistical analysis was also conducted on these data to understand its significance. Two-way analysis of variance (ANOVA) was used to investigate main effects and interaction effects (Table V).

Table VI: ANOVA Analysis of Parameter Effect on Recast Thickness

<i>Source</i>	<i>P-Value</i>
<i>Voltage</i>	0.001
<i>Pulse On-Time</i>	0.015
<i>Interaction Effects</i>	0.203

At  $\alpha=0.05$ , the voltage and pulse on-time main effects are statistically significant and the interaction effects are not significant. This indicates that the factors do not interact to produce effects not already predicted by the main effects.

## IV. Discussion

### i. Microhardness

Due to the instantaneous melting and quenching process that occurs at the surface during EDM, it was hypothesized that the recast layer hardness would be significantly different from the base material. This was only the case for the samples below the maximum voltage.

All the recast layers below the maximum voltage were softer than the base material. This is most likely due to the precipitation hardenable nature of 15-5 stainless steel. As received, the sample had been aged to a higher hardness. Upon re-solidification at the surface, the material was most likely closer to the annealed state, leading to it being softer than the base material. However, it is possible that the steel was instead over-aged. However, this would make it softer as well.

Being significantly different in hardness to the base material would lead to changes in the mechanical properties between the two, leading to reduced performance in service life. While a softer steel generally has more favorable fatigue properties, the fatigue life of steel is greatly dependent on its surface condition, meaning the recast layer would reduce fatigue life. As seen in the microhardness tests along the recast layer, it also fractures extremely easily under a low applied load. Again, this would reduce the service life of the part considerably.

While there is no doubt that the presence of the recast layer is detrimental to mechanical properties, there were multiple issues with the microhardness tests performed in this study.

Firstly, the SEM images of the microhardness tests near the recast layer showed a difference in the amount of area the indenter was indenting; it was indenting less area near the recast layer, meaning the area near the recast layer was harder than the base material. If the recast layer was truly softer than the base material, the portion of the indenter diamond closer to the recast layer would indent more area, not less. Secondly, tests directly on the recast layer may have produced softer readings due to the microcracking and porosity present in the recast layer. When indented, the microcracks easily propagate and fail, leading to less force required by the indenter to indent the material, resulting in reduced hardness readings.

A final flaw of the tests is the size of the indenter. The indenter is larger than the recast layer, meaning tests would always include some amount of base material or nickel plating, no matter how well aimed. Therefore, the microhardness measurements do not agree with the scanning electron microscope images and it is not possible to fully conclude that the recast layer is indeed significantly different in hardness when compared to the base material. To produce more accurate results, nanohardness testing would be more appropriate.

## ii. Recast Layer Thickness

Recast layer measurements suggests a reduction in recast layer thickness as both testing parameters were reduced. This is expected, as a decreased voltage and pulse on-time produces a lower overall energy input. However, the interaction of the two is not significant in producing a smaller recast layer. This is most likely due to the way the parameters were reduced. A reduction of 25% for peak voltage is a much larger reduction than the same in pulse on-time. As the two parameters are reduced together, decrease in voltage becomes the controlling variable.

The recast thickness values were typically less than values reported by prior studies, especially because previous studies had a much larger heat affected zone than seen in this study. This means that less material needs to be removed with a secondary machining process. The rough nature of the layer implies negative effects on mechanical properties. The recast layer also contains a significant amount of residual stresses due to the rapid cooling which contribute to the lessened mechanical properties as well. Although decreased recast layer thickness means less surface material requires removal, defects present in the layer are nevertheless harmful. SEM

imaging depicted large voids and microcracks visible throughout the recast layer (Figure 13). These defects are sites in which cracks can propagate through the material, causing premature fracture and failure. Variability in the thickness of the recast layer can be observed here – just a few microns at the base of the image, increasing to a local maximum of about ten microns.

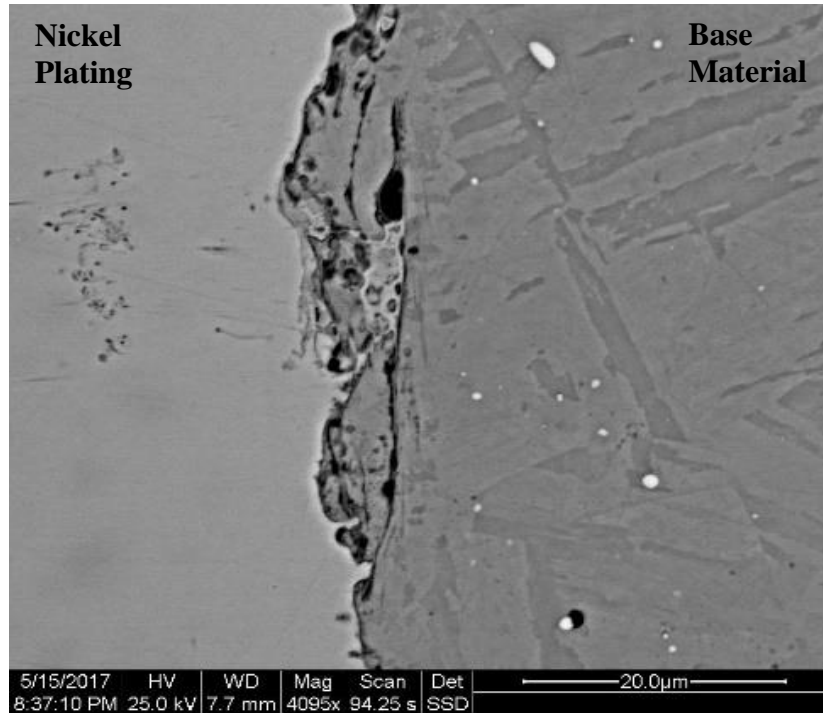


Figure 13: A 13 μs, 8V sample exhibits variability in recast layer thickness.

The roughness of the recast layer also presents an issue in corrosive environments. These voids can act as craters in which pitting and crevice corrosion will readily occur.<sup>18</sup> These counteract the effects of the stainless steel, which is typically extremely resistant to both types of corrosion due to the passive oxide layer. With the combination of reducing the corrosion resistance as well as the mechanical properties, the recast layer still needs to be removed.

No evidence of a significant heat affected zone was present. There was no grain coarsened region visible, and little local melting at grain boundaries. Similar to the small size of the recast layer, this is due to the low energy input of the EDM process. Only a small amount of material at the surface is heated to a temperature hot enough to be vaporized, resulting in the negligible size of the heat affected zone observed in this study. While the energy density of the process is high, the energy input is not sustained long enough to significantly alter material below. The area affected by the sparking is small, and after the material is removed, dielectric fluid rushes into the cavity produced by the vacating material. This allows for a significant amount of heat transfer to occur

with the dielectric fluid, preventing all the heat input to the material from being transferred further. This cooling process does produce the defect filled recast layer, but controls the damaging of the workpiece to the surface, instead of penetrating deeper into the material. Therefore, after removal of the recast layer, a short heat treatment should be sufficient to fully restore the steel to a sufficiently homogeneous state.

## V. Conclusions

1. A reduction in the pulse on-time on the EDM machine yields a smaller recast layer due to reduced energy input.
2. Lowering the EDM machine voltage parameter also yields a smaller recast layer.
3. The EDM recast layer has a rough surface and contains many voids, pores, and microcracks.

## Works Cited

1. "15-5 PH Stainless Steel" AK Steel. Web.
2. "Best Stainless & Alloys." Web. <<http://www.beststainless.com/valve-manufacturing.html>>.
3. Boeing. "Fatigue Properties of 17-4 PH and 15-5 PH Steel in the H-900 and H-1050 Condition." Dtic.mil: Web. 27 Aug. 1969.
4. DiMatteo, Nikki D. ASM Handbook: Vol. 19: Fatigue and Fracture. Ed. Steven R. Lampman. Alexandria, VA, United States: ASM International, 1996. Print.
5. Ashby, "Chapter 17: Fatigue Failure," Engineering Materials.
6. "MMPDS-03: Metallic Materials Properties Development and Standardization." *Introduction and Steel Alloys 1* (2007).
7. Jameson, Elman C. Electrical Discharge Machining. Dearborn, MI: Society of Manufacturing Engineers, 2001. Print.
8. Chen, "Surface Integrity and Fatigue Performance of Inconel 718 in Wire Electrical Discharge Machining" *Procedia CIRP* 45 (2016): 307-310.
9. "Wire EDM Image." Web. <<https://4.bp.blogspot.com>>.
10. Puri, A.B., and B. Bhattacharyya. "Modeling and Analysis Of White Layer Depth In A Wire-Cut EDM Process Through Response Surface Methodology." *International Journal of Advanced Manufacturing Technology* 25.3/4 (2005): 301-307.
11. Imran, M., et al. "Assessment of Surface Integrity of Ni Superalloy After Electrical-Discharge, Laser And Mechanical Micro-Drilling Processes." *International Journal of Advanced Manufacturing Technology* 79.5-8 (2015): 1303-1311.
12. Mower, Todd M. "Degradation of Titanium 6Al-4V Fatigue Strength Due to Electrical Discharge Machining." *International Journal of Fatigue* 64. (2014): 84-96
13. Kiyak, Murat, Bilal Aldemir, and Erhan Altan. "Effects of Discharge Energy Density on Wear Rate And Surface Roughness In EDM." *International Journal of Advanced Manufacturing Technology* 79.1-4 (2015): 513-518.



14. Newton, Thomas R., et al. "Investigation of The Effect Of Process Parameters On The Formation And Characteristics Of Recast Layer In Wire-EDM Of Inconel 718." *Materials Science & Engineering: A* 513-514. (2009): 208-215.
15. Klocke, F., et al. "Structure and Composition of the White Layer in the Wire-EDM Process." *Procedia CIRP* 42 (2016): 673-678.
16. Amorim, F. L., & Weingaertner, W. L. Die-sinking electrical discharge machining of a high-strength copper-based alloy for injection molds. *Journal of the Brazilian Society of Mechanical Sciences and Engineering*, 26(2), (2004). 137-144.
17. Lee, H. T., and C. Liu. "Calibration of Residual Stress Measurements Obtained From EDM Hole Drilling Method Using Physical Material Properties." *Materials Science & Technology* 24.12 (2008): 1462-1469. Academic Search Premier. Web. 10 Feb. 2017.
18. Khalaj Amineh, Sasan, et al. "Improving the Surface Quality in Wire Electrical Discharge Machined Specimens by Removing the Recast Layer Using Magnetic Abrasive Finishing Method." *International Journal of Advanced Manufacturing Technology*, vol. 66, no. 9-12, June 2013, pp. 1793-1803.